

An image difference metric based on simulation of image detail visibility and total variation

Marius Pedersen

The Norwegian Colour and Visual Computing Laboratory, Gjøvik University College (Norway).

Abstract

Many image quality and image difference metrics have been proposed over the last decades. An important factor when evaluating the image quality or image difference is the viewing distance. In this paper we propose a new image difference metric based on the simulation of detail visibility and total variation. The simulation of detail visibility by using shearlets takes into account the viewing conditions and the viewing distance, and calculation of the image difference is done by total variation. Evaluation has been carried out to verify the simulation of image detail visibility, and it is showing promising results. Evaluation of the new image difference metric is also promising.

Introduction

It is well-known that when moving further away from a natural image some information become imperceptible. This imperceptible information can, with good benefit, be discarded, and only the perceptible information is preserved. The removal of imperceptible information can be beneficial in image compression, halftoning, gamut mapping, and image quality evaluation. In this paper we will focus on the latter. It has been shown that image quality and image difference metrics incorporating features of the human visual system are more robust than those who do not [1]. Several methods have been proposed to mimic the visual system [2–6], and some specifically to simulate image detail visibility [7, 8]. Many of these methods have been incorporated into image quality and difference metrics [4, 6, 8, 9], and these metrics have been shown to correlate with perceptual judgments [6, 8, 10].

A recent method to simulate image detail visibility was proposed by Pedersen and Farup [8]. This method is based on a wavelet decomposition of the image. However, wavelets are not good at representing discontinuities, which are commonly found in natural images. This limitation of wavelets has resulted in many new approaches for decomposition, such as directional wavelets [11], complex wavelets [12], ridgelets [13], curvelets [14] and contourlets [15]. All of these have the main idea to contain basis elements with many more shapes and directions than the wavelet bases. Pedersen et al. [7] used contourlets to extend the method to simulate image detail visibility, replacing wavelets with contourlets. However, a drawback of using contourlets is that artifacts can be introduced [16].

Shearlets is a rather new class of multidimensional representation systems, which was introduced by Labate et al. [17]. By applying different actions as dilation, shear transformation and translation to a fixed function we can obtain

shearlets. It exhibits many advantageous geometric and mathematical properties, for example directionality, elongated shapes, scales, and oscillations. One advantage of this approach over other approaches is that it can be constructed using a generalized multi-resolution analysis and implemented very efficiently. Shearlets are, due to their analytic and geometric properties, capable of capturing precisely the geometry of edges [18].

In this paper we propose a new image difference metric based image detail visibility and Total Variation (TV). First we improve the simulation of image detail visibility by extending the method proposed by Pedersen and Farup [8] to use shearlets. Then we incorporate this improved simulation method in an image difference metric based on TV.

The paper is organized as follows: First we introduce relevant background, then we present the new method for simulation of image detail visibility and the new image difference metric. Further, we evaluate the simulation and the metric, at last we conclude and present future work.

Background

Pedersen et al. [6] proposed a color image difference metric based on the work of Peli [5] and TV. In this method image detail visibility simulation is done through the use of a pyramidal image-contrast structure where for each frequency band, the contrast is defined as the ratio of the bandpass-filtered image at the frequency to the low-pass filtered image at an octave below the same frequency. This is filtered in the CIEXYZ color space using the Contrast Sensitivity Functions (CSFs) from Peli [19] and Johnson and Fairchild [2] for luminance and chrominance, respectively. The filtered images are then converted to the log-compress OSA-UCS color space, as proposed by Oleari et al. [20]. The Total Variation of Difference (TVD) metric is defined as:

$$TVD = TV + \lambda CD, \quad (1)$$

where TV related to the difference in details, λ is a weighting parameter, and CD is the Euclidean color difference.

Pedersen and Farup [8] extended the image detail visibility simulation further by decomposing the image with wavelets. The images were transformed into a new color space inspired by the YC_bC_r , then a wavelet composition was carried out to obtain a octave width bands of frequencies. They also selected the luminance CSF from Barten [21], since it incorporated the luminance level. The chromatic CSFs were obtained from Johnson and Fairchild [3]. In addition, contrast masking was accounted for by using the

extended intra channel masking model accounting for local activity as described by Nadenau [22]. Then the simulated images were used as input to the TVD metric in Equation 7. The proposed metric showed increased performance compared to using filtering from S-CIELAB [4].

Another improvement of the detail visibility simulation was proposed by Pedersen et al. [7]. In this work the wavelets decomposition was exchanged with the non-subsampled contourlet, and the luminance CSF was the one proposed by Barten [23] that incorporate orientation dependence of the CSF and the effect of surround illumination. This combination resulted in a more precise simulation of detail visibility compared to using wavelets.

Proposed Image Difference Metric: Total Variation of Difference

The proposed image difference metric follow the general framework of low-level based metrics, with a transformation into a suitable color space, then filtering with a model simulating the human visual system, before calculation of image difference, and at last pooling [10].

Color space transformation

We start by transforming the image into the Ybr color space as proposed by Pedersen and Farup [8]. A sRGB input image is assumed, which is linearized to remove the gamma correction. The linear RGB image is transformed into to CIEXYZ, and further into a new RGB space. In this new RGB space the primaries are defined to match the wavelengths of the monochromatic gratings used in the measurements of the chromatic CSFs [24]. Red is defined as 602 nm, green 526 nm, and blue 470 nm. Then the image is transformed into the new Ybr color space using the following equation:

$$Y = Y_r R + Y_g G + Y_b B, \quad (2)$$

where $R, G,$ and B are the new linear RGB values, $Y_r, Y_g,$ and Y_b are the \bar{y} values from the color-matching functions for the red, green, and blue channels, such that Y is the CIE luminance. The color channels are defined as:

$$b = \frac{Y_b B}{Y} \quad \text{and} \quad r = \frac{Y_r R}{Y}.$$

Since the channel contrasts in the new color space correspond exactly to contrast definitions used by Mullen [24], we can apply the CSF curves directly. Another advantage of this color space, is that the channels are decorrelated.

Image detail simulation

Further, we follow the idea proposed by Peli [5], where a decomposition of the image carried out and the contrast between the bandpass and lowpass information is calculated. Each of the three color channels are decomposed using shearlets¹. Unless stated otherwise the images have been decomposed at four scales, with 2, 3, and 4 shear levels, otherwise standard parameters have been used. After

¹We have used the Matlab implementation of shearlets, ShearLab 3D V1.0, from <http://www.shearlab.org/>, visited 26/03/14

decomposition we obtain a set of lowpass filtered coefficients (LL), and several sets of highpass coefficients from different levels, shearings, and cones. We then filter the highpass coefficients with CSFs, in which a luminance CSF is applied to the achromatic channel (Y) and chrominance CSFs to the chromatic channels (b and r). Shearlets also have the advantage of division into different orientations, therefore we use the luminance CSF from Barten [23] that include orientation dependence and surround illumination:

$$CSF_L(u) = \frac{C \exp\left(-0.0016u^2(1+100/L)^{0.08}\right)}{\sqrt{\left(1 + \frac{144}{X_0^2} + 0.64(1+3\sin^2(2\varphi)u^2)\left(\frac{63}{L^{0.83}} + \frac{1}{1-\exp^{-0.02u^2}}\right)\right)}}, \quad (3)$$

where C is a constant adapted to the CSF measurements. Barten [23] reports values from 3700 to 5800 for C depending on the measurements. We used a value of 3700, as Pedersen et al. [7]. u is the spatial frequency in cycles per degree, L is the luminance in cd/m^2 , and X_0^2 is the angular object area in square degrees, and φ is the orientation angle in degrees. A multiplicative correction factor, f , is used to account for that the visibility of an object can change depending of the surround, as proposed by Barten [23]:

$$f = \exp\left(-\frac{\ln^2\left(\frac{L_s}{L}\left(1 + \frac{144}{X_0^2}\right)^{0.25}\right) - \ln^2\left(\left(1 + \frac{144}{X_0^2}\right)^{0.25}\right)}{2\ln^2(32)}\right), \quad (4)$$

where L is the luminance of the object, L_s is the surround luminance, and X_0^2 is the object area in square degrees of visual angle. This is the same luminance CSF as used by Pedersen et al. [7].

For the chrominance CSF, two CSFs are required, one for the red-green channel and one for the blue-yellow channel. We apply the CSFs from Johnson and Fairchild [3]:

$$CSF_C = \alpha_1 \exp(-\beta_1 u^{\gamma_1}) + \alpha_2 \exp(-\beta_2 u^{\gamma_2}), \quad (5)$$

where u is defined as cycles per degree and the parameters for the red-green and blue-yellow channels are given by Table 1, as given by Johnson and Fairchild [3].

Table 1: Parameters for the chrominance CSFs from Johnson and Fairchild [3].

Parameter	red-green channel	blue-yellow channel
α_1	109.14130	7.032845
β_1	-0.00038	-0.000004
γ_1	3.42436	4.258205
α_2	93.59711	40.690950
β_2	-0.00367	-0.103909
γ_2	2.16771	1.648658

The luminance CSF (CSF_L) is applied to the luminance channel (Y), and the chrominance CSFs (CSF_C) are applied to the chrominance channels (b and r) for each level, cone, and shearing. The CSFs are not normalized and applied directly at the given scale.

Now, let $l'_j(x, y)$ denote the contrast filtered LL band and $h_{\psi\tau j}(x, y)$ denote the highpass bands (depending on the shearing ψ and cone τ) at level j . At the lowest level, the LL band is not filtered, thus $l'_N(x, y) = l_N(x, y)$, where N denotes the lowest level. Furthermore, let $a_{\psi\tau j}(x, y)$ denote the CSF filtered version of $h_{\psi\tau j}(x, y)$ as described above. Then, the contrast filtered octave bands are defined as

$$h'_{\psi\tau j}(x, y) = \begin{cases} h_{\psi\tau j}(x, y) & \text{if } a_{\psi\tau j}(x, y) > l'_j(x, y) \\ 0 & \text{else} \end{cases} \quad (6)$$

The filtered information in ψ shears (orientations) and τ cones are then used to reconstruct the image to obtain the lowpass filtered version for the next level. In addition, we also incorporate contrast masking as done by Pedersen et al. [7] using the extended intra channel masking model accounting for local activity as described by Nadenau [22].

Quality calculation and pooling

The quality calculation is carried out in a similar manner as proposed by Pedersen et al. [6]. After the filtering, the original and reproduction are converted to the log-compressed OSA-UCS color space as proposed by Oleari et al. [25]. This color space is chosen since perceived differences have shown to correlate well with calculated differences [26]. The Total Variation of Difference (TVD) is calculated using the following equation:

$$TVD = \sqrt{\sum_j \left(\int_{\Omega} |\nabla L_{O_j} - \nabla L_{R_j}| dA \right)^2} + \lambda \int_{\Omega} \sqrt{\sum_j (L_{O_j} - L_{R_j})^2} dA, \quad (7)$$

where $\sqrt{\sum_i (\int_{\Omega} |\nabla L_{O_i} - \nabla L_{R_i}| dA)^2}$ is the TV term, while $\lambda \int_{\Omega} \sqrt{\sum_j (L_{O_j} - L_{R_j})^2} dA$ is the Color Difference (CD) term. L_O is the original filtered image and L_R its filtered reproduction. Ω is the image domain, λ is the weighting parameter for the CD term, and j indicates the color channel. The TV term is similar to the color TV defined by Blomgren and Chan [27], except that the gradient of the difference between the original and reproduction is taken, and the CD term is the Euclidean color difference.

Evaluation of proposed detail visibility simulation

The original and simulated image should be indistinguishable if they are viewing from the simulated distance or further away. If viewed at a distance closer than the simulated distance they should be distinguishable. In the first case the information that has been removed from the simulated image is the same information that is imperceptible in the original. It is also important that simulation does not introduce artifacts, both since the artifacts can be perceptible at the simulated distance or further away, but also to keep the image quality when the simulated image is viewed at a closer distance than the simulated distance. Two different evaluations have been carried out; a visual investigation and a subjective experiment.

Visual investigation

One drawback of contourlets is artifacts [16], and in order to evaluate if the proposed method introduces artifacts in the simulated images we carry out a visual investigation. We use a test target, the same as in Pedersen et al. [7], for evaluation. The target has been filtered with the proposed shearlet method and the contourlet method (Figure 1). We can see that the proposed method has less visible artifacts compared to using contourlets. The contourlet method produce false coloring around the edges, and this is greatly reduced or not visible by using shearlets.

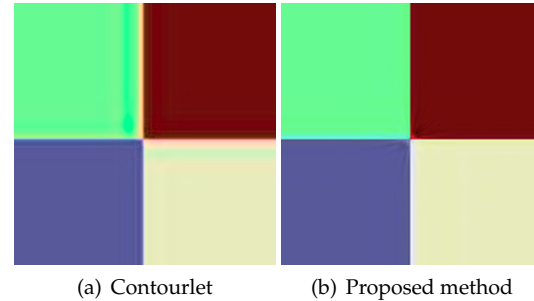


Figure 1. Test target for the evaluation of artifacts (simulated 2 meter). The image has been enlarged to show the artifacts. We can see that the proposed method has fewer artifacts around the edges than the contourlet method.

Figure 2 shows the image detail visibility simulation at a distance of 4 meters compared to the original. We can see that the proposed method has removed the noise and created a "softer" image, but it preserves the main structures and edges of the image. Figure 3 shows a cutout of a natural image simulated with the contourlet method (top) and the proposed shearlets methods (bottom). The contourlet method have more prominent ringing artifacts compared to shearlets, especially on the left side of the image.

Subjective experiment

Experimental setup

The experiment was carried out as a forced-choice paired-comparison with flipping of the pairs. The observer viewed the simulated image and the original at 2 and 4 meters. Their task was to indicate which one of the images that were blurred and/or contained artifacts. Six different scenes were used (Figure 4), all 512×512 pixels. The images were simulated according to the viewing distance with using shearlets and contourlets. Comparison was only done

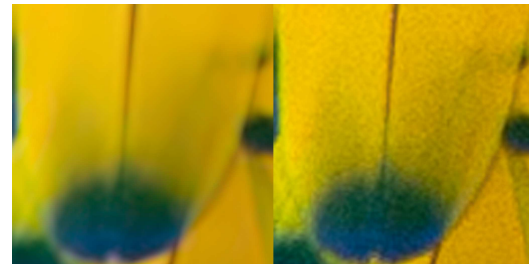


Figure 2. Comparison of a region between a simulated image at 4 meters and the original. The image has been enlarged to enhance the differences.



Figure 3. Comparison of a region between contourlets (top) and shearlets (bottom). The contourlet method has more prominent ringing artifacts compared to shearlets. The image has been enlarged to enhance the differences.



Figure 4. Images used for the evaluation of the proposed method.

against the contourlet method, since it has shown to outperform other methods [7]. The images were shown on an Eizo ColorEdge CG246 monitor, calibrated to sRGB. The monitor luminance was set to 80 cd/m², according to the sRGB specification. The surround illumination (D50) was set to approximately 20 lux. 14 observers participated in the experiment, who all passed a visual acuity test and with normal color vision. Since all observers saw each pair twice, a total of 28 observations per pair were recorded.

Data analysis

For each distance the percentage of correct identifications of the simulated image was calculated. If the method works as expected, a 75% correct identification rate should be obtained at the given simulate distance [8, 19]. 95% confidence intervals have been calculated as Wilson score interval with continuity correction [28].

Results

The results for all images for the new method using shearlets and contourlets is shown in Figure 5. The method based on shearlets have an identification rate of 64% at 4 meters, while at 2 meters it has a identification rate of 76% and with a 95% confidence interval overlapping the desired identification rate of 75%. The contourlet method has an identification rate of 47% at 4 meters and 57% at 2 meters, and the 95% confidence interval does not overlap the desired 75% identification rate at the two distances. Investigation of the results for the individual results show that

the confidence intervals for proposed method overlaps the desired 75% identification rate for all six test images at 2 meters, and in three of the six images at 4 meters. It also has more stable rates for the entire test set compared to the contourlet method. Observers commented that in some images it was difficult or impossible to identify the content of the images at 4 meters. This could influence the results since the observers indicated that they were more comfortable answering when they were able to identify the content of the images.

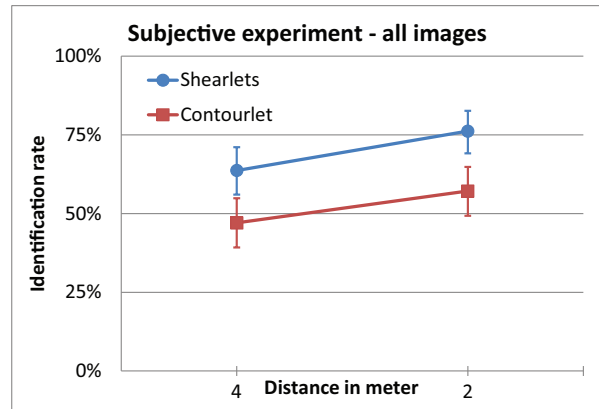


Figure 5. Identification rates with 95% confidence intervals for the proposed method using shearlets and the previous method using contourlets. 168 observations have been made for each method.

Evaluation of the image difference metric

Experimental setup

For evaluation of the proposed metric we select two databases where the viewing distance and the viewing conditions have been carefully controlled. The Colourlab Image Database:Image Quality (CID:IQ) [29] contains 23 pictorial images, and we select different distortions from CID:IQ; JPEG compression, JPEG2000 compression, Poisson Noise, Gaussian Blur and SGCK gamut mapping. The originals images have been modified over 5 levels for each distortion. The subjective results from 17 subjects were gathered at two viewing distances; 100cm and 50cm.

In addition we have used the dataset from Ajagamelle et al. [30]. It contains a total of 80 images, where ten are original images which have been modified in contrast, lightness, and saturation. 14 observers judged the perceived difference between the original and the reproductions from a distance of 70 cm, forming the basis for the observer scores.

As a performance indicator the linear Pearson and Spearman correlation between the metric scores and observer quality scores has been calculated for each original image. This is done because there are scale differences between the images [31], making it better to individually analyze images than an overall evaluation. In addition to the TVD metric with the proposed image detail visibility simulation we have also calculated the TVD metric without this simulation. If the proposed simulation method improves the performance then we should see higher correlations for the TVD with the simulation compared to the TVD without.

We will show the results for $\lambda = 0.5$.

Results

Results for the average Pearson correlation for 23 images is shown in Figure 6. Due to the page limitation we cannot show the individual results per image. We can see that for both metrics, with and without simulation, produces high correlation coefficients for both viewing distances and the different distortions. For JPEG2000 and SGCK at 50cm, JPEG and JPEG2000 at 100cm, the proposed metric has the highest correlation values. It is also positive that it improves the correlation for JPEG at 100cm, which has the lowest correlation of all distortions. For JPEG at 50cm, Poisson at 100cm and Gaussian blur the metric without simulation has a slightly higher correlation coefficient. The two metrics are similar for Poisson noise at 50cm. Overall, both metrics perform quite well, having correlation values above 0.8. It is natural that both metrics follow a similar trend, since the quality calculation is identical.

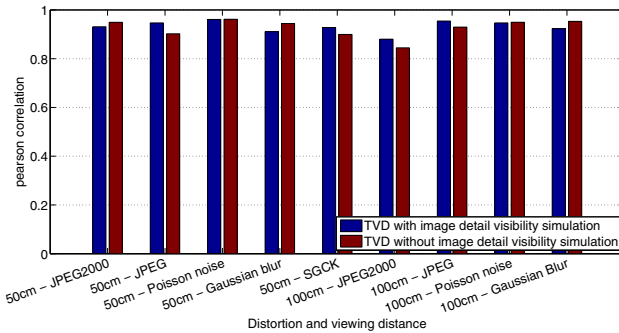


Figure 6. Average Pearson correlation for 23 images for different distortions in the CID:IQ database for 50cm and 100cm viewing distance.

Analysis of the Spearman correlation for the CID:IQ distortions show that for both 50cm and 100cm viewing distance the proposed metric has a slightly higher mean Spearman correlation for the JPEG compressed images, for the Gaussian blur distortoin the metric without simulation has a slightly higher correlation coefficients, while for the two other distortions the correlation value is identical between TVD with and without simulation. The Spearman correlation values are very high, which indicates that the metric is capable of giving the same rank order as the observers.

Figure 7 shows Pearson correlation values for each of the original images in the Ajagamelle dataset. We can see that TVD with image detail visibility simulation improves the correlation slightly in four worst images, while for the remaining six images it has a similar or slightly worse correlation. Investigation of the Spearman correlation coefficients shows that the TVD with simulation has a better performance in 5 images, identical in 2, and worse in 3 images. Also for Spearman the worst correlation coefficient is improved.

Discussion

TVD without simulation of image detail visibility has a very good performance, and it is difficult to improve an

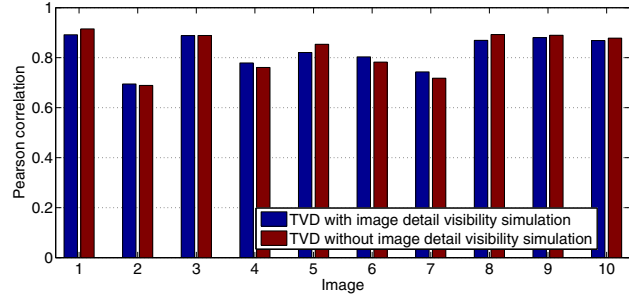


Figure 7. Pearson correlation for the Ajagamelle dataset.

already well-performing metric. However, the results indicate that by incorporation of a simulation of image detail visibility can be beneficial, but additional evaluation on more difficult datasets is required.

It is positive that the TVD with simulation of image detail visibility is increasing the correlation for the worst performing distortions. It also increases the performance for the gamut mapping distortions, which has been a difficult challenge for image difference metrics [32].

It is worth noting that the correlation values are not statistically significantly different, for either of the databases. For a given specific condition the TVD without simulation could be sufficient for estimating image difference, without the added complexity of the image detail simulation. However, there are situations where the viewing distance and viewing conditions would significantly influence the judgement of image difference (or image quality), where the proposed method would give better results.

Conclusion

We have proposed a new image difference metric based on total variation and simulation of image detail visibility. Evaluation of the image detail visibility show promising results, with less artifacts compared to previous method and better agreement with observers. Evaluation of the proposed image difference metric is promising, but additional evaluation is required. Comparison against other state of the art image difference metrics remains as future work.

Acknowledgment

The author would like to thank Prof. Ivar Farup for his generous advice, helpful comments and suggestions. This research has been funded by the Research Council of Norway over the SHP programme.

References

- [1] P. Le Callet and D. Barba. A robust quality metric for color image quality assessment. In *International Conference on Image Processing (ICIP)*, volume 1, pages 437–440, Barcelona, Spain, Sep 2003. IEEE.
- [2] G. M. Johnson and M. D. Fairchild. On contrast sensitivity in an image difference model. In *Image Processing, Image Quality, Image Capture, Systems Conference (PICS)*, pages 18–23, Portland, OR, Apr 2002.
- [3] G. M. Johnson and M. D. Fairchild. Darwinism of color

- image difference models. In *Color Imaging Conference*, pages 108–112, Scottsdale, AZ, Nov 2001.
- [4] X. Zhang and B. A. Wandell. A spatial extension of CIELAB for digital color image reproduction. In *Soc. Inform. Display 96 Digest*, pages 731–734, San Diego, CA, 1996.
- [5] E. Peli. Contrast in complex images. *J. Opt. Soc. Am. A*, 7:2032–2040, 1990.
- [6] M. Pedersen, G. Simone, M. Gong, and I. Farup. A total variation based color image quality metric with perceptual contrast filtering. In *International conference on Pervasive Computing, Signal Processing and Applications*, Gjøvik, Norway, Sep 2011.
- [7] M. Pedersen, X. Liu, and I. Farup. Improved simulation of image detail visibility using the non-subsampled contourlet transform. In *Color and Imaging Conference*, pages 191–196, Albuquerque, NM, USA, Nov. 2013. IS&T.
- [8] M. Pedersen and I. Farup. Simulation of image detail visibility using contrast sensitivity functions and wavelets. In *Color and Imaging Conference*, pages 70–75, Los Angeles, CA, November 2012.
- [9] G. M. Johnson and M. D. Fairchild. A top down description of S-CIELAB and CIEDE2000. *Color Research and Application*, 28(6):425–435, December 2003.
- [10] M. Pedersen and J. Y. Hardeberg. Full-reference image quality metrics: Classification and evaluation. *Foundations and Trends in Computer Graphics and Vision*, 7(1): 1–80, 2012.
- [11] J.-P. Antoine, R. Murenzi, and P. Vandergheynst. Directional wavelets revisited: Cauchy wavelets and symmetry detection in patterns. *Applied and Computational Harmonic Analysis*, 6(3):314 – 345, 1999.
- [12] N. Kingsbury. Complex wavelets for shift invariant analysis and filtering of signals. *Applied and Computational Harmonic Analysis*, 10(3):234 – 253, 2001.
- [13] E. J. Cands and D. L. Donoho. Ridgelets: a key to higher-dimensional intermittency? *Philosophical Transactions of the Royal Society of London. Series A:Mathematical, Physical and Engineering Sciences*, 357 (1760):2495–2509, 1999.
- [14] E. J. Candes and D. L. Donoho. Curvelets a surprisingly effective nonadaptive representation for objects with edges. In C. Rabut, A. Cohen, and L.L. Schumaker, editors, *Curves and Surfaces*. Nashville, TN, Vanderbilt University Press, 2000.
- [15] M.N. Do and M. Vetterli. The contourlet transform: an efficient directional multiresolution image representation. *IEEE Transactions on Image Processing*, 14(12):2091–2106, dec. 2005.
- [16] G. Kutyniok, W-Q. Lim, and X. Zhuang. Digital shearlet transforms. In G. Kutyniok and D. Labate, editors, *Shearlets*, Applied and Numerical Harmonic Analysis, pages 239–282. Birkhauser Boston, 2012.
- [17] D. Labate, W-Q. Lim, G. Kutyniok, and G. Weiss. Sparse multidimensional representation using shearlets. In M. Papadakis, A. F. Laine, and M. A. Unser, editors, *Wavelets XI*, volume 5914, pages 59140U–59140U–9, San Diego, CA, Jul. 2005. SPIE.
- [18] K. Guo, D. Labate, and W-Q. Lim. Edge analysis and identification using the continuous shearlet transform. *Applied and Computational Harmonic Analysis*, 27(1):24 – 46, 2009.
- [19] E. Peli. Contrast sensitivity function and image discrimination. *Journal of the Optical Society of America A*, 18(2):283–193, 2001.
- [20] C. Oleari, M. Melgosa, and R. Huertas. Euclidean color-difference formula for small-medium color differences in log-compressed OSA-UCS space. *Journal of the Optical Society of America A*, 26(1):121–134, 2009.
- [21] P. G. J. Barten. *Contrast sensitivity of the human eye and its effect on image quality*, chapter 3, pages 25–64. HV Press, 1999.
- [22] M. Nadenau. *Integration of human color vision models into high quality image compression*. PhD thesis, École Polytechnique Fédérale de Lausanne, 2000.
- [23] P. G. J. Barten. Formula for the contrast sensitivity of the human eye. In Y. Miyake and D. R. Rasmussen, editors, *Society of Photo-Optical Instrumentation Engineers (SPIE) Conference Series*, volume 5294, pages 231–238, December 2003.
- [24] K. T. Mullen. The contrast sensitivity of human colour vision to red-green and blue-yellow chromatic gratings. *The Journal of Physiology*, 359:381–400, 1985.
- [25] C. Oleari, M. Melgosa, and R. Huertas. Euclidean color-difference formula for small-medium color differences in log-compressed OSA-UCS space. *Journal of the Optical Society of America A*, 26(1):121–134, 2009.
- [26] D. R. Pant and I. Farup. Riemannian formulation and comparison of color difference formulas. *Color Research & Application*, 37(6):429–440, Dec 2012.
- [27] P. Blomgren and T. F. Chan. Color TV: Total variation methods for restoration of vector-valued images. *IEEE Transactions on Image Processing*, 7(3):304–309, Mar 1998.
- [28] R. G. Newcombe. Two-sided confidence intervals for the single proportion: comparison of seven methods. *Statistics in Medicine*, 17(8):857–872, 1998.
- [29] X. Liu, M. Pedersen, and J.Y. Hardeberg. Cid:iq - a new image quality database. In A. Elmoataz, O. Lezoray, F. Nouboud, and D. Mammass, editors, *Image and Signal Processing*, volume 8509 of *Lecture Notes in Computer Science*, pages 193–202. Springer International Publishing, Cherbouurg, France, Jul. 2014.
- [30] S. A. Ajagamelle, M. Pedersen, and G. Simone. Analysis of the difference of gaussians model in image difference metrics. In *5th European Conference on Colour in Graphics, Imaging, and Vision (CGIV)*, pages 489–496, Joensuu, Finland, Jun 2010. IS&T.
- [31] M. Pedersen and J. Y. Hardeberg. Rank order and image difference metrics. In *4th European Conference on Colour in Graphics, Imaging, and Vision (CGIV)*, pages 120–125, Terrassa, Spain, Jun 2008. IS&T.
- [32] J. Y. Hardeberg, E. Bando, and M. Pedersen. Evaluating colour image difference metrics for gamut-mapped images. *Coloration Technology*, 124(4):243–253, Aug 2008.